



XXXVII IBERIAN LATIN AMERICAN CONGRESS
ON COMPUTATIONAL METHODS IN ENGINEERING
BRASÍLIA - DF - BRAZIL

COMPRESSED AIR ENGINE WITH ACTIVE CONTROL UNDER PRESSURE SATURATION IN THE CONTROL OF OSCILLATING ROTATION

Alexandre de Castro Alves

alexandre.alves.unesp@gmail.com

UNESP – São Paulo State University, Faculty of Mechanical Engineering, Av. Engenheiro Luiz Edmundo Carrijo Coube, 14-01, 17.033-360, Vargem Limpa, Bauru, São Paulo, Brazil.

Angelo Marcelo Tusset

tusset@utfpr.edu.br

UTFPR – Federal Technological University of Parana, Department of Electronics, Av. Monteiro Lobato, s/n-km 04, 84.016-210, Ponta Grossa, Paraná, Brazil.

Jose Manoel Balthazar

jmbaltha@gmail.com / jmbaltha@ita.br

UNESP – São Paulo State University, Faculty of Mechanical Engineering, Av. Engenheiro Luiz Edmundo Carrijo Coube, 14-01, 17.033-360, Vargem Limpa, Bauru, SP, Brazil and ITA – Aeronautics Technological Institute, Mechanical Aeronautics Division, Praça Marechal Eduardo Gomes, 50, 12.228-900, Vila das Acacias, São José dos Campos, São Paulo, Brazil.

Rodrigo Tumolin Rocha

digao.rocha@gmail.com

UNESP – São Paulo State University, Faculty of Mechanical Engineering, Av. Engenheiro Luiz Edmundo Carrijo Coube, 14-01, 17.033-360, Vargem Limpa, Bauru, São Paulo, Brazil.

Frederic Conrad Janzen

fcjanzen@utfpr.edu.br

UTFPR – Federal Technological University of Parana, Department of Electronics, Av. Monteiro Lobato, s/n-km 04, 84.016-210, Ponta Grossa, Paraná, Brazil.

Abstract. *This work evaluates the oscillating rotation of a connecting-rod-crank mechanism as compressed air engine with input saturation control. The mechanism positions are controlled with a non-conservative excitement by air pressure that controls the positions of the angular output. It is evaluated the control of the angular position through the command by pneumatic valve controlled by the method of control. Initially applies control without restricting the maximum pressure that achieves saturation pressure in response to the control function. Therefore, must be limited maximum pressure in the input at 1MPa for the application and control in industrial pneumatic equipment. Thus, it analyzes the parametric error for the angular position relative to the desired control, with and without saturation function. However, when applying the saturation control function checks that the system becomes stable despite the parametric error increase at one decimal place of 10^{-3} to 10^{-2} . Therefore, the parametric errors obtained are suitable and can be applied to control the angular oscillation of the output to the compressed air engine as a stable system by controlling the saturation.*

Keywords: *input saturation, nonlinear system, nonlinear dynamics, connecting-rod-crank*

1 INTRODUCTION

The target of the control of mechanical systems is to generate a consistent behavior between the actuation and response through the application of an output control function. In this control engineering appears a phenomenon known as saturation, which occurs mainly in the application of real physical variables based on their characteristics and limitations. Therefore, the saturation of this manipulated variable can provide inadequate results for the control, which can lead to instability. In this way, several recent works address the saturation control variable and discusses ways to obtain a stable and controllable system (Askari et al., 2016, Wang et al., 2016; Zheng & Sun, 2016, Oravec & Bakošová, 2015; Wang et al., 2013).

These control systems can be implemented in various mechanical mechanisms, machines or manufacturing process equipment, to convert rotary movements into translational or vice versa. Using this type of motion conversion has several studies for control the connecting-rod-crank mechanism, in the majority to control the linear position of the translational movement as output (Ahmad et al., 2011; Chuang et al., 2006; Chuang, 2007; Fung et al., 2009; Kao et al., 2006; Lin et al., 2001; Liermann et al, 2016). However, few studies assess the conversion of rotary movements into translational using active controls (Yu et al., 2016; Hung et al. 2016). These types of work use passive controls for continuous movement of rotation, for use as compressed air motors or hydropneumatic (Shi et al., 2016; Yu & Cai, 2015; Brown et al., 2014; Wang et al, 2014; Shaw et al., 2013).

This connecting-rod-crank mechanism provides movement of oscillating for active control of the output shaft as engine compressed air. The analysis of this swinging motion control provides condition for applications in mechanical devices such as manufacturing process and agricultural machinery. The engine compressed air and your movements should be evaluated because of clean energy that provides advantages to be applied to certain types of processes and equipment. In this context, we also have studies to the application of pneumatic energy for use in automotive vehicles (Yu et al, 2016; Hung et al 2016) in which the connecting-rod-crank already established itself as the main mechanism.

2 CONTROL FOR THE DYNAMIC MODEL

The mechanism of compressed air engine has a geometry comprising a system with four links rigid that makes up the connecting-rod-crank. The mechanism of compressed air engine has a geometry comprising a system with four links rigid that makes up the connecting-rod-crank. The movement between the links of the mechanism depends on these restrictions for the transmission of forces applied to the Centers of Gravity (CG) in each link.

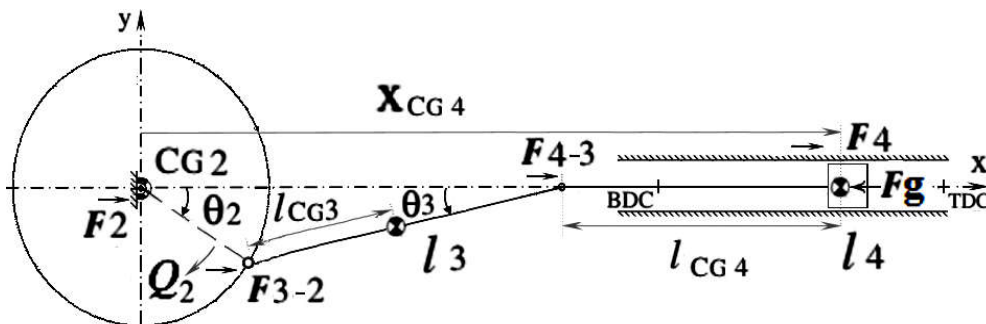


Figure 1 - Connecting-rod-crank with horizontal geometry

where

- l_i = total length of the link l_i ;
- l_{CGi} = length of the link l_i to CG;
- x_{CG4} = linear position of CG cylinder 4 to the origin;
- θ_i = angular position of the link l_i ;
- F_i = viscous friction force between the links l_i ;

The kinematic relationship which describes between the input and output movement of mechanism with a degree of freedom in function of their positions can be written, as follows.

$$x_{CG4} = l_2 \cos \theta_2 + (l_3^2 - l_2^2 \sin^2 \theta_2)^{1/2} + l_{CG4} \quad (1)$$

We note that the nonlinear dynamic in this mechanism is a function of the angular positions in link 2 obtained for the input motions in the link 4. In connecting-rod-crank mechanism as combustion engine some authors modeling (Awrejcewicz & Kudra, 2003) this mechanism as triple physical pendulum with barriers which generating six piston movements from one side of the cylinder to the other. This configuration generates three degree of freedom for the motion creates a more real model but much more complex. For model simplification in our work was considered only one degree of freedom, as shown in the following Fig.1. Through the gas force application (F_g) in the link 4 in function of pneumatic pressure. For the control of the air pressure variation in the input link 4 applies F_g in both directions for a dual action in the cylinder.

To apply the control movement in the mechanism we can model dynamics through Lagrangian mechanics in which measures the conservative energy of this system, based on generalized coordinate θ_2 , as follows.

$$\frac{d}{dt} \left(\frac{\partial \mathcal{L}}{\partial \dot{\theta}_2} \right) - \frac{\partial \mathcal{L}}{\partial \theta_2} = Q_{\theta_2} \quad (2)$$

where

- Q_{θ_2} = moment of non-conservative forces related to generalized coordinate θ_2 ;
- $\mathcal{L} = T - V$;
- T = kinetic energy;
- V = potential energy;
- θ_2 = angular position of link 2;
- $\dot{\theta}_2$ = angular velocity of link 2;

Thus, we have the difference between the kinetic and potential energy, as follows.

$$\mathcal{L} = \frac{1}{2} ((J_2 \dot{\theta}_2^2) + (m_3 v_3^2 + J_3 \dot{\theta}_3^2) + (m_4 v_4^2)) - \frac{1}{2} (m_3 g l_3 \sin \theta_3). \quad (3)$$

where

- m_i = concentrated mass in link CG i ;
- v_i = velocity of link i ;
- J_i = momentum of inertia of link i ;
- θ_i = angular position of link i ;
- $\dot{\theta}_i$ = angular velocity of link i ;

2.1 Control LQR

To apply the Q_{Ui} control signal in LQR control system in Eq. (4) need vary the air pressure in a proportional P_{Ui} pressure control valve which generates the force F_g (Fig. 1) a function of coordinated variation of the generalized, as follows.

$$Q_{Ui} = F_{gi} \left(\frac{\partial x_{CG4}}{\partial \theta_2} \right) = P_{Ui} (\pi d^2 / 4) (-l_2 \sin^2 x_1 - (l_2^2 \sin x_1 \cos x_1) / (l_3^2 - l_2^2 \sin^2 x_1)^{1/2}) \quad (5)$$

where

P_{Ui} = control pressure case i ;

d = diameter of the cylinder 4;

F_{gi} = control variable force case i ;

However, to perform numerical simulations will need to define the overall control function for Q_{Ui} . According to Tusset et al. (2013) to apply LQR linear control in Eq. (4) of movement we need have linearized the non-linear equation for the following format.

$$\dot{\mathbf{X}} = \mathbf{A}\mathbf{X} + \mathbf{B}\mathbf{U} \quad (6)$$

where

$$\mathbf{X} = [x_1 \quad x_2]^T;$$

$\mathbf{A}_{n \times n}$ = state matrix;

$\mathbf{B}_{n \times m}$ = constant matrix;

$\mathbf{U} = Q_{Ui}$ = the control signal;

This form of equation and the gains for the implementation of LQR method include the obtainment for linearized motion equation. Thus, to linearize the nonlinear model will need obtain the equilibrium point type and verify to your applying for the non-linear model in question for LQR method. This analysis was performed in Alves et al. (2015) that determined the equilibrium point $\mathbf{P} = (-\pi/2, 0)$, i.e., we have as equilibrium a stable focus point which will be converted on matrix \mathbf{A} .

$$\mathbf{A} = \begin{bmatrix} 0 & 1 \\ -40.8333 & -0.4167 \end{bmatrix} \quad (7)$$

In this case, the sign of the control \mathbf{U} can used to as the application in the linear model as in the nonlinear model, to the positioning in the desired orbit increasing. That is, $\mathbf{U} = Q_{Ui}$ increases the system power according to the increase of air pressure to the control point and can be obtained from:

$$\mathbf{U} = -\mathbf{R}^{-1}\mathbf{B}^T\mathbf{P}\mathbf{Z} \quad (8)$$

where

$$\mathbf{Z} = \begin{bmatrix} x_1 - x_1^* \\ x_2 - x_2^* \end{bmatrix};$$

x_1^* e x_2^* = desired position and velocity;

Assuming that $\mathbf{P}_{(nxn)}$ is the solution for the Riccati equation given by:

$$\mathbf{A}^T \mathbf{P} + \mathbf{P} \mathbf{A} - \mathbf{P} \mathbf{B} \mathbf{R}^{-1} \mathbf{B}^T \mathbf{P} + \mathbf{Q} = \mathbf{0} \quad (9)$$

where

\mathbf{Q}_{nxn} and \mathbf{R}_{nxm} are positive semi-definite matrices.

However, the controllability matrix $[\mathbf{B} \ \mathbf{A}\mathbf{B} \ \dots \ \mathbf{A}^{(n-1)}\mathbf{B}]$ must have full rank and the choice of matrix must be made appropriately to be not violated the controllability of the system.

This way, the matrices \mathbf{B} , \mathbf{Q} and \mathbf{R} are determined, in the following, to the solution of Riccati's equation.

$$\mathbf{B} = \begin{bmatrix} 0 \\ 1 \end{bmatrix}; \mathbf{Q} = \begin{bmatrix} 5(10^7) & 0 \\ 0 & 5(10^7) \end{bmatrix}; \mathbf{R} = [10^{-4}]; \quad (10)$$

By applied the matrices \mathbf{A} , \mathbf{B} , \mathbf{Q} and \mathbf{R} on the Riccati's Eq. (7) \mathbf{P} is obtained.

$$\mathbf{P} = \begin{bmatrix} 1000.9381 & 3.121 \\ 3.121 & 3.1628 \end{bmatrix} \quad (11)$$

Substituting the matrix \mathbf{P} in Eq. (11), we have the Eq. (12) to the control signal \mathbf{U} that when applied in Eq. (7), it controls the linear motion.

$$Q_{Ui} = \mathbf{U} = -707065.9490(x_1 - x_1^*) - 707107.3644(x_2 - x_2^*) \quad (12)$$

Thus, there were obtained the Eq. (12) for general control function $\mathbf{U} = Q_{Ui}$ for apply in the Eq. (6) with the aim to control the linear motion. However, the movement equation for this study is a nonlinear Eq. (4) for can use the linear LQR gains by possessing equilibrium point with stable focus.

For the solution in Equation (4) of movement nonlinear will need use the control signal \mathbf{U} described in the Eq. (12) that was obtained by linearization of Eq. (6) of motion around its equilibrium point. This application and analysis of LQR control results for a nonlinear equation can be developed because of the type of equilibrium condition for the connecting-rod-crank system that meets control laws.

2.2 Numerical simulations

To control x_1^* we have to formulate the objective function with the frequency and the limits the desired control position, in a way to obtain the smallest parametric error in positioning ($e_{Ui} = x_i - x_i^*$), as follows.

$$x_1^* = (\pi/2)\cos(8.26t) - (\pi/2) \quad (14)$$

$$x_2^* = -(\pi/2)8.26\sin(8.26t) \quad (15)$$

Therefore, the control equation below expresses the control function for the mechanism through the combinations of Eq. (12), (14) and (15), as follows.

$$Q_{Ui} = \begin{pmatrix} -707065.9490(x_1 - (\pi / 2 \cos(8.26 t) - \pi / 2)) \\ -707107.3644(x_2 + (\pi / 2(8.26) \sin(8.26 t)) \end{pmatrix} \quad (16)$$

In the analysis of saturation have to check if the pressure limit was not exceeded with relation to the control signal value generated in Eq. (12), and if it happens we have to restrict the signal against this maximum pressure.

Thus, we have three cases to be evaluated, in the first case 1 does not impose itself a limit to the pressure which creates saturated control pressure Q_{U1} . In case 2 will need to restrict the maximum limit for application of pressure control signal P_{U2} on 1 MPa so that there is not saturation pressure in the application of the control signal Q_{U2} , as follows. In the case 3 is also considered the uncertain errors of 20% (Noziaki, Balthazar & Tusset, 2013) to the application of the LQR control as a variation of the previous function, as follows.

$$Q_{U1 \text{ or } U2 \text{ or } U3} = Eq.(12) \text{ (case 1 or 2 or 3)}$$

$$P_{U1 \text{ or } U2 \text{ or } U3} = \frac{Q_{U1 \text{ or } U2 \text{ or } U3}}{(\pi d^2 / 4)(-l_2 \sin^2 x_1 - (l_2^2 \sin x_1 \cos x_1) / (l_3^2 - l_2^2 \sin^2 x_1)^{1/2})}$$

$$\text{if } abs(P_{U2 \text{ or } U3}) > 1.00 \text{ (only in case 2 or 3)}$$

$$Q_{U2} = \frac{abs(P_{U2})}{P_{U2}} \left(\frac{\pi d^2}{4} \right) (-l_2 \sin^2 x_1 - (l_2^2 \sin x_1 \cos x_1) / (l_3^2 - l_2^2 \sin^2 x_1)^{1/2})$$

$$Q_{U3} = (Q_{U2}) \cdot 1.0 + (Q_{U2}) \cdot 0.1 \cdot Rand \text{ (random number ranging between -1, 0 and 1)}$$

else

end

(17)

However, the angular positions desired, x_j^* and x_j , should vary from 0 to $-\pi$ around the balance point $-\pi / 2$. In all following figures these angular positions are presented in real scale, in radians (rad).

The other variables are normalized between -1 and 1, being necessary to multiply the values in the figures to obtain the values of variables, P_{Ui} (Mpa), Q_{Ui} (N.m) and e_{Ui} (rad). To

the simulations, it was used the following physical parameters to the connecting-rod-crank mechanism as shown in the table.

Table 1. Parameters to the connecting-rod-crank mechanism

Constitutive relation	Nomenclature	Value	Unit
Angular position	θ_2	0 to $-\pi$	rad
Cylinder stroke	Δl_{CG4}	0.056	m
Crankshaft length	l_2	0.04	m
Connecting-rod length	l_3	0.2	m
Crankshaft mass	m_2	1.0	kg
Connecting-rod mass	m_3	0.5	kg
Cylinder mass	m_4	0.5	kg
Viscous-damping of the compressed air engine	c_{cae}	0.01	N.m.s / rad
Viscous-damping of the equipment	c_{eq}	1.0	N.m.s / rad
Cylinder diameter	d	0.05	m

In case 1 in Fig. 2, 3,4 and 5 below were obtained the following values for numerical simulations of normalized variables without pressure restraint, $Q_{UI} = 856.3$ N.m, $P_{UI} = 5.61$ MPa and $e_{UI} = 0.0022$ rad.

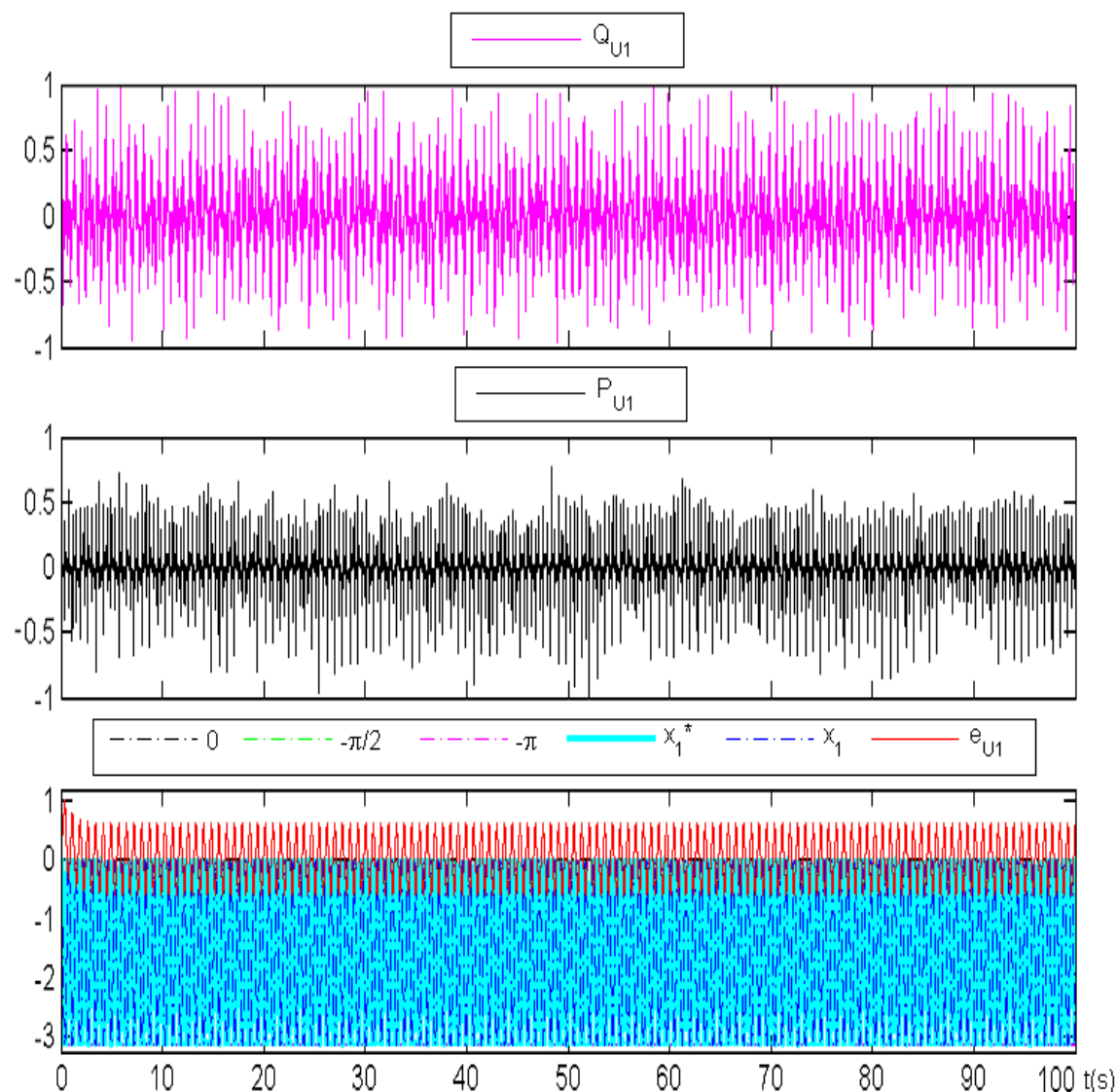


Figure 2 - LQR active control without restriction of the maximum pneumatic pressure

Analyzing the Figure below the amplified case it can be observed that according to the initial condition the biggest error $e_{U1} = 0.0022$ rad occurs at the beginning of the transient regime.

However, this error generated by the control function applied in the Eq. (12) generates pressures that reach peaks up to 5.61 MPa. Therefore, the pressure becomes saturated for practical application, when it exceeds the value for the pressure 1 MPa, which would not be viable for the utilization in commercial pneumatic equipments.

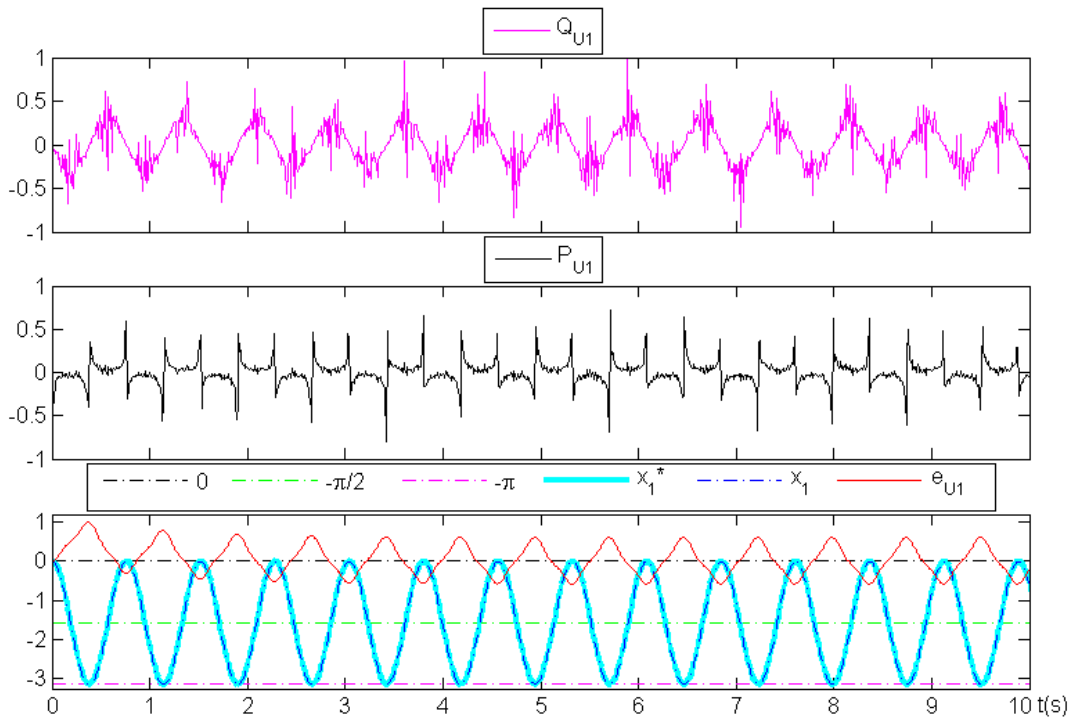


Figure 3 - LQR active control without restriction pressure and amplified at the transient regime

In Figure 4 below show up the last ten seconds of the case 1 of Fig. 2 without pressure restriction for analysis of the variables in permanent regime.

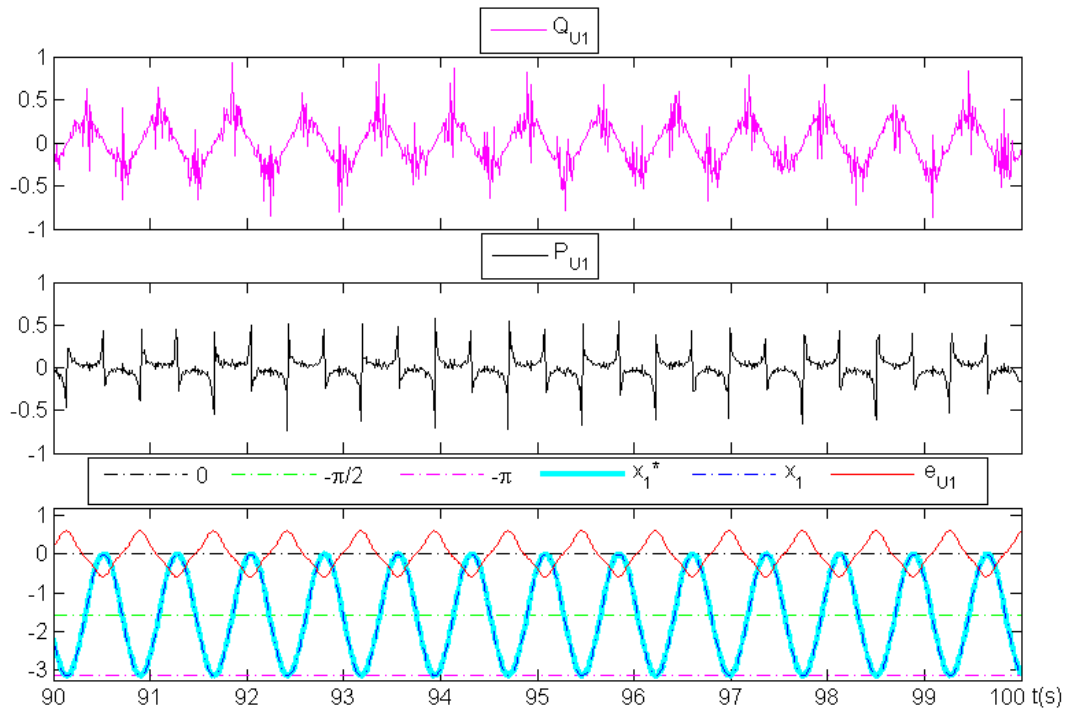


Figure 4 - LQR active control without restriction pressure and amplified at the permanent regime

It can be seen in Fig. 4 and Fig. 5 which in the permanent regime the parametric error decreases to $e_{U1} = 0.0013$ rad, because in this stage the position no receives large influence of the initial condition.

However, even maintaining the same initial condition of the case 1, in the case 2 according to the maximum pressure limitation $P_{U2} = 1$ MPa occurs an increase in the maximum error parametric for $e_{U2} = 0.0275$ rad with increasing at one decimal place for the radians as shown in the Fig. 5.

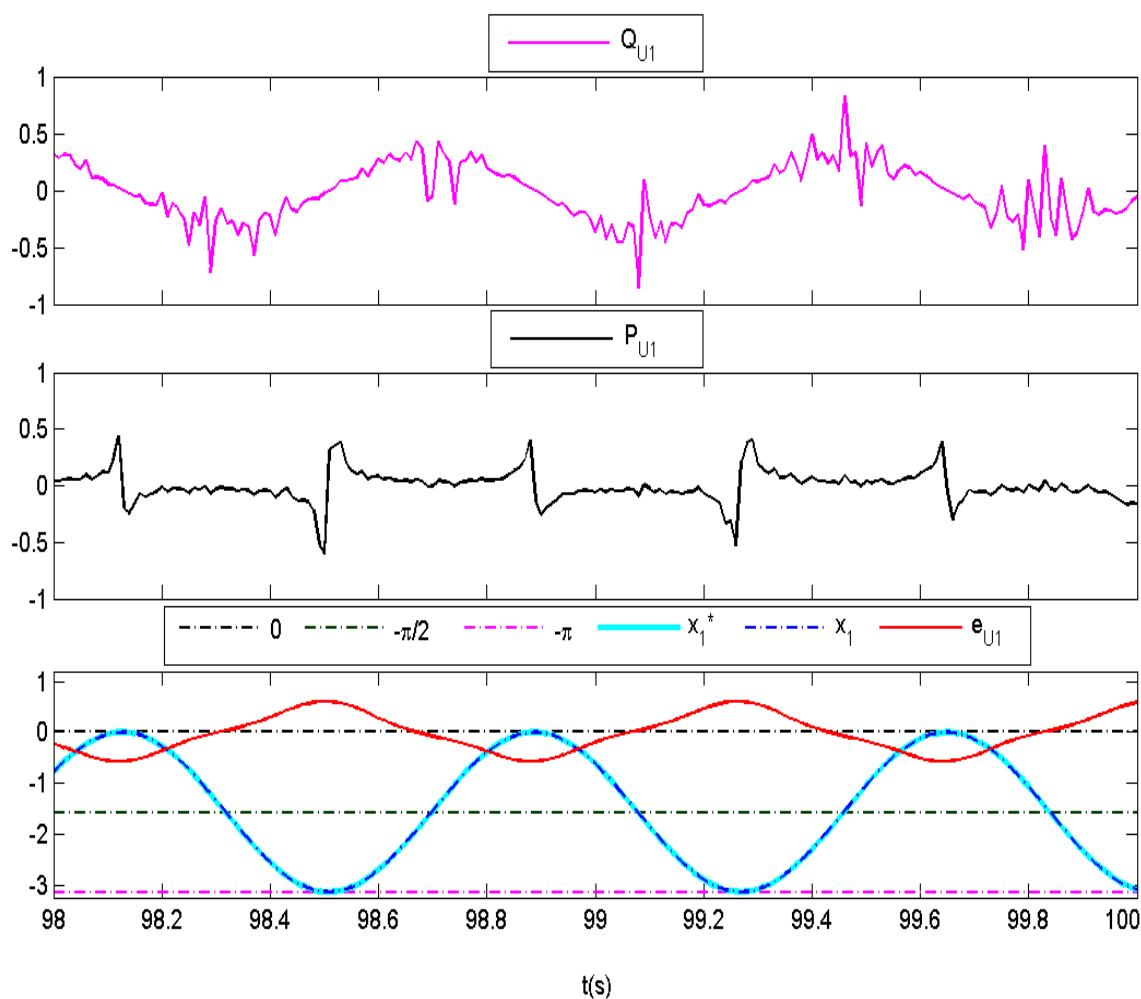


Figure 5 - LQR active control with the saturated pressure in the permanent regime to analysis the peaks of the controlled variables

In Fig. 5 above we can see that due to the lack of restriction occurs spikes of pressure saturated every time we have which reverse the crank oscillating movement. However, after these peaks most of the time we have values a little above zero for the pressure, i. e., the positions are controlled with small pressure for most of the control system.

In case 2 in Fig. 6, 7, 8 and 9 below were obtained the following values for numerical simulations of normalized variables without pressure restraint, $Q_{U2} = 801.0$ N.m, $P_{U2} = 1.00$ MPa and $e_{U2} = 0.0275$ rad.

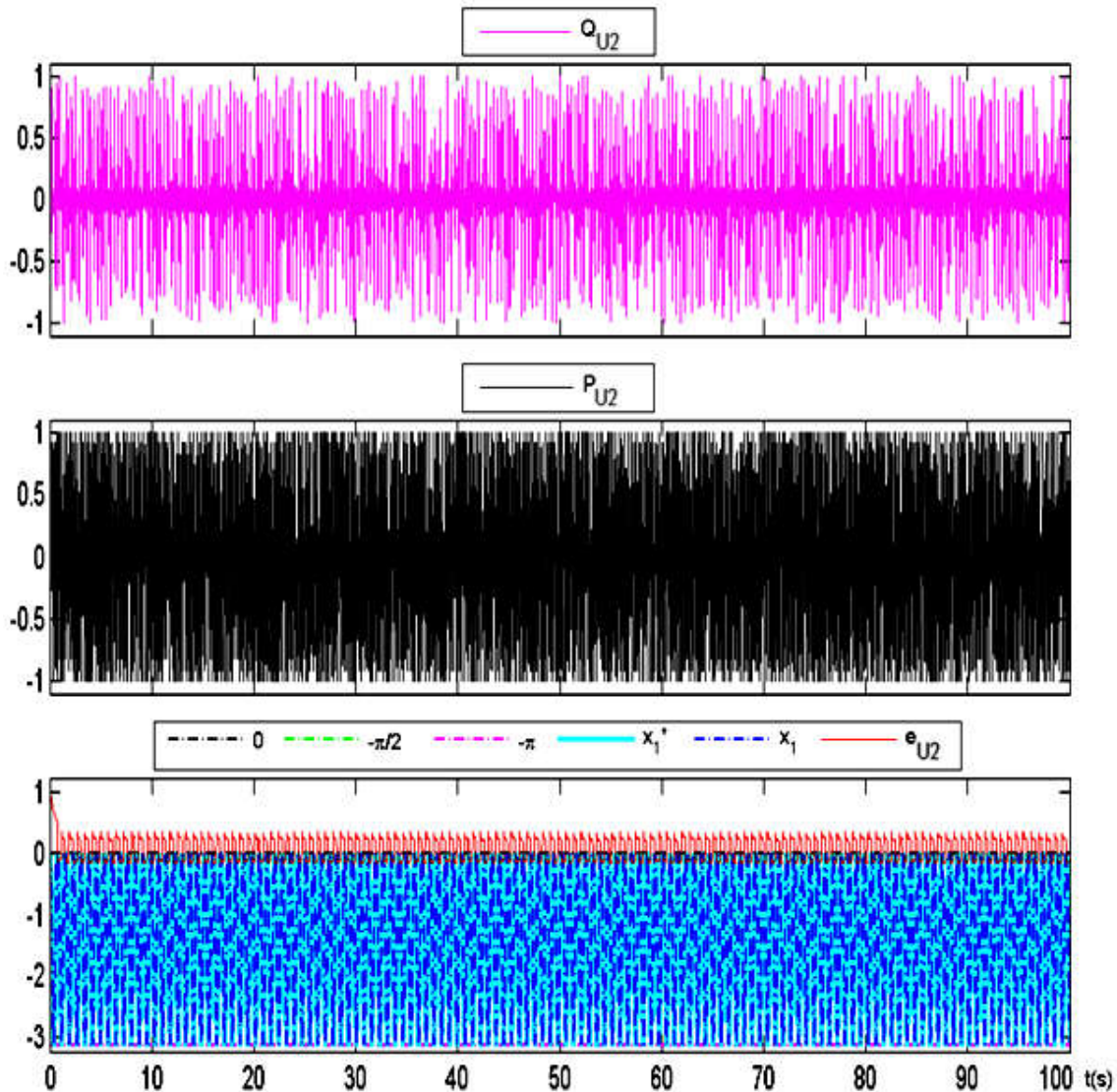


Figure 6 - LQR active control with restriction of the maximum pneumatic pressure

In case 1 in Fig. 2, 3, 4 and 5 previous were obtained the following values for numerical simulations of normalized variables with pressure restraint, $Q_{U2} = 801.0$ N.m, $P_{U2} = 1.00$ MPa and $e_{U2} = 0.0275$ rad. Thus, it can be seen in Fig. 6 for the case 2 amplified that besides increasing the parametric error on 10^1 of 2.22×10^{-3} for 2.75×10^{-2} compared to the case 1. Occurs also the reduction the moment of non-conservative force of excitement $Q_{U1} = 856.3$ to $Q_{U2} = 801.0$ N.m with these values already expected due to the control pressure with restriction at $P_{U2} = 1$ MPa.

In Figure 7 below for the case 2 amplified verified that this limitation for the pressure enables its practical application on commercial pneumatic equipments. Thus, for the correction of the position x_1 through of the control function verifies that which no saturation occurs because the pressure signal remains constant in some parts of the movement.

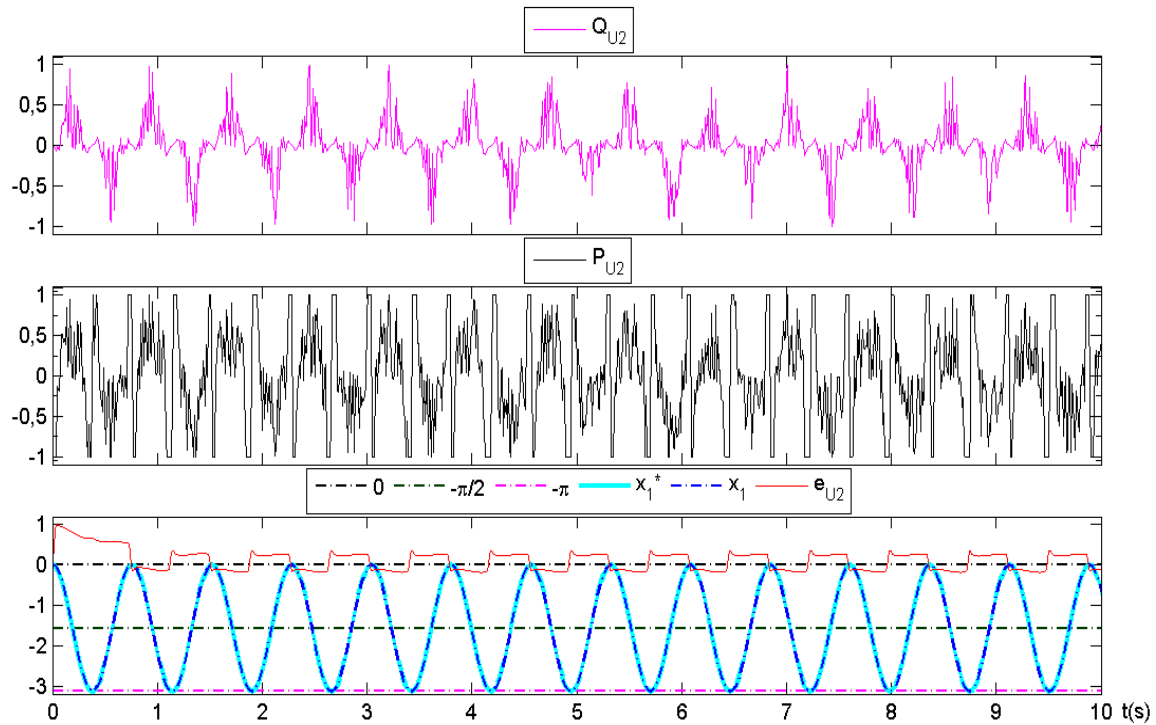


Figure 7 - LQR active control with restriction pressure and amplified at the transient regime

In Figure 8 below show up the last ten seconds of the case 2 of Fig. 6 without pressure restriction for analysis of the variables in permanent regime.

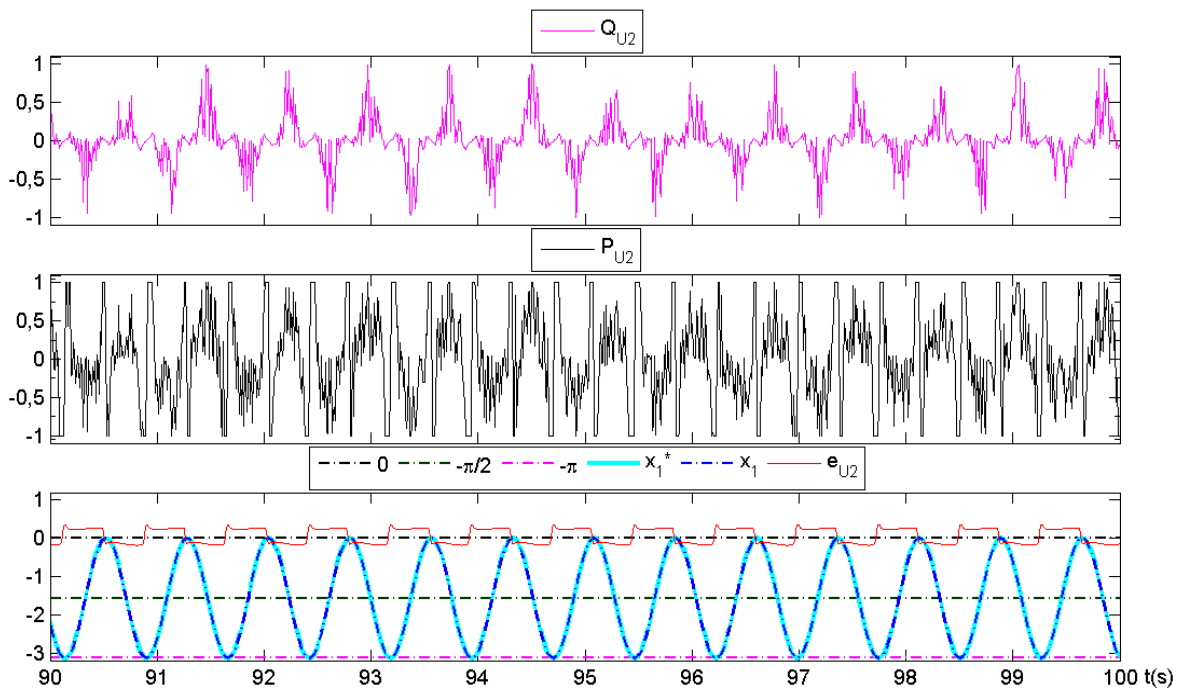


Figure 8 - LQR active control with restriction pressure and amplified at the permanent regime

In case 2 in the permanent regime with the pressure restriction it is observed the decrease of parametric error for $e_{U2} = 0.0097$ compared to the beginning of the transient regime that generates the error maximum $e_{U2} = 0.0275$ rad.

Comparing the errors for case 1 e 2 Fig. 9 below in the permanent regime it is verified which, for both cases with (Fig. 5) and without restriction it is had an actual increase of 0.0084 in the parametric error between cases, increasing $e_{U1} = 0.0013$ for $e_{U2} = 0.0097$ rad.

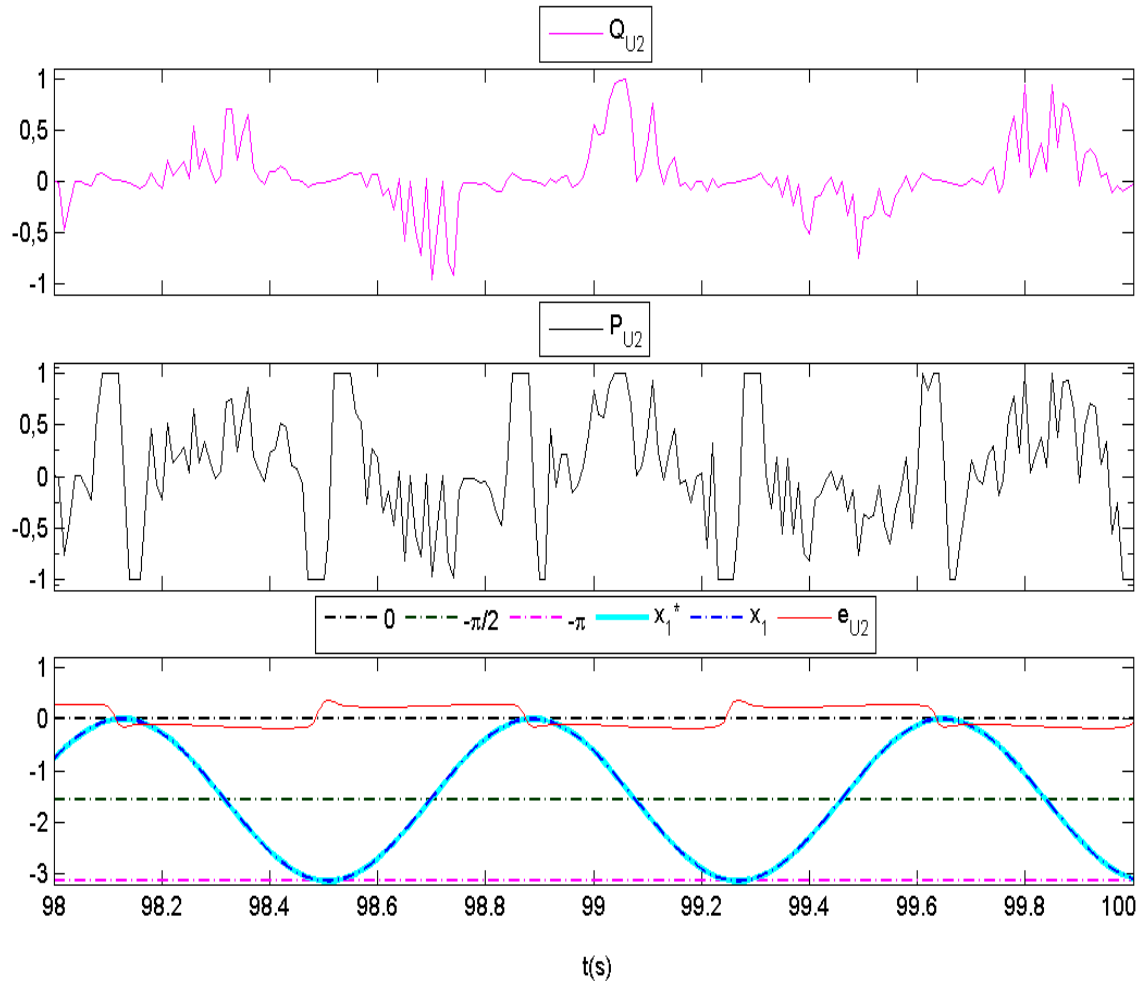


Figure 9 - LQR active control without the saturated pressure and without noise in the permanent regime for the analysis the peaks of the controlled variables

In Fig. 9 above for the case 2, we can see that due to limitation of maximum pressure we obtained peaks that are constant, i.e., each time we it happens the reversal of the oscillating motion of the crank. However, these peaks occur most of the time because do not have more peaks with saturated pressures as occurs and can seen in Fig. 5 for the case 1.

In case 3 in Fig. 10, 11, 12 and 13 below were obtained the following values for numerical simulations of normalized variables without pressure restraint, $Q_{U3} = 881.0$ N.m, $P_{U3} = 1.10$ MPa ranging 10% above or below the pressure maximum proposed for 1.10 MPa and $e_{U3} = 0.0028$ rad.

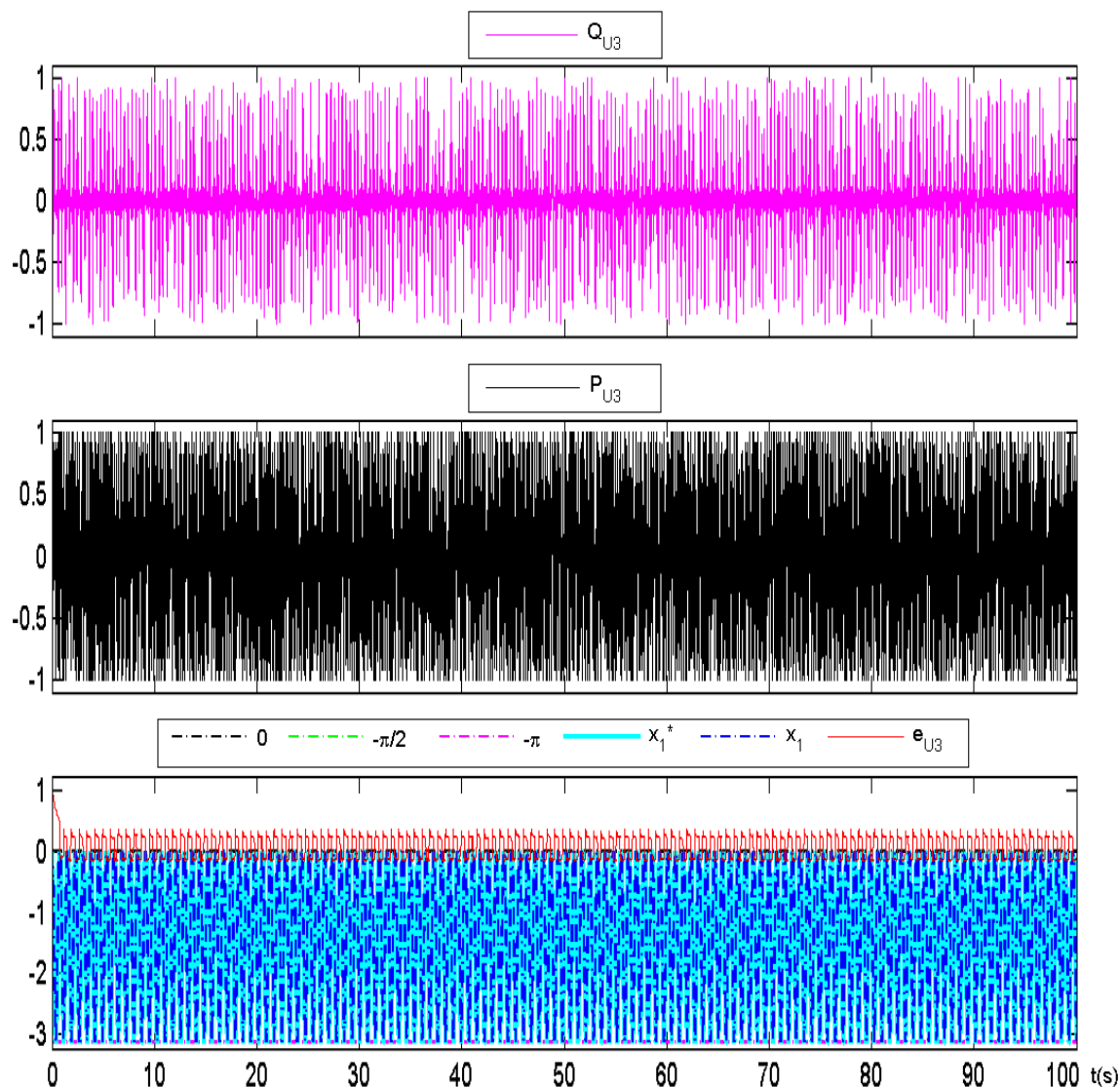


Figure 10- LQR active control with noise and with restriction of the maximum pressure

In next Fig. 11 below show up the last ten seconds of the case 3 of Fig. 10 without pressure restriction for analysis of the variables in permanent regime. In this case 3 a function of noise in the input pressure, there was increase in the maximum Q_{U3} (881.0) to compensate the shorter time in the maximum pressure when compared with the case 2 Q_{U2} (801.3) without noise.

The error in the transient and permanent regime same considering uncertainties in the values of pressure, such as the compressibility of the fluid, differences in the friction values, vibrations and noises remained virtually the same error comparing it with the case 3.

For the case 3 in the next Fig. 11, it appears that because of the uncertainties for the maximum pressure the peaks are no longer constant as in the previous case, which can be verified in saw shape thereof, both in permanent regime and transient.

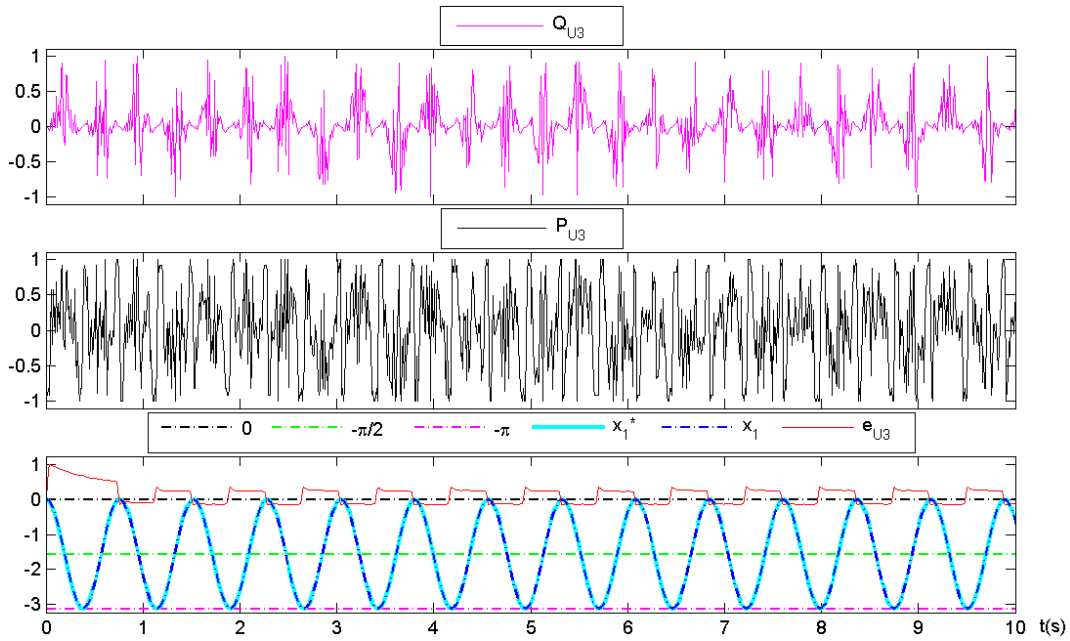


Figure 11 - LQR active control with restriction, noise, uncertainties, amplified at the transient regime

In case 3 for the permanent regime in the Fig. 12 it is observed the decrease of parametric error for $e_{U3} = 0.0099$ compared to the beginning of the transient regime that generates the error maximum $e_{U3} = 0.0280$ rad.

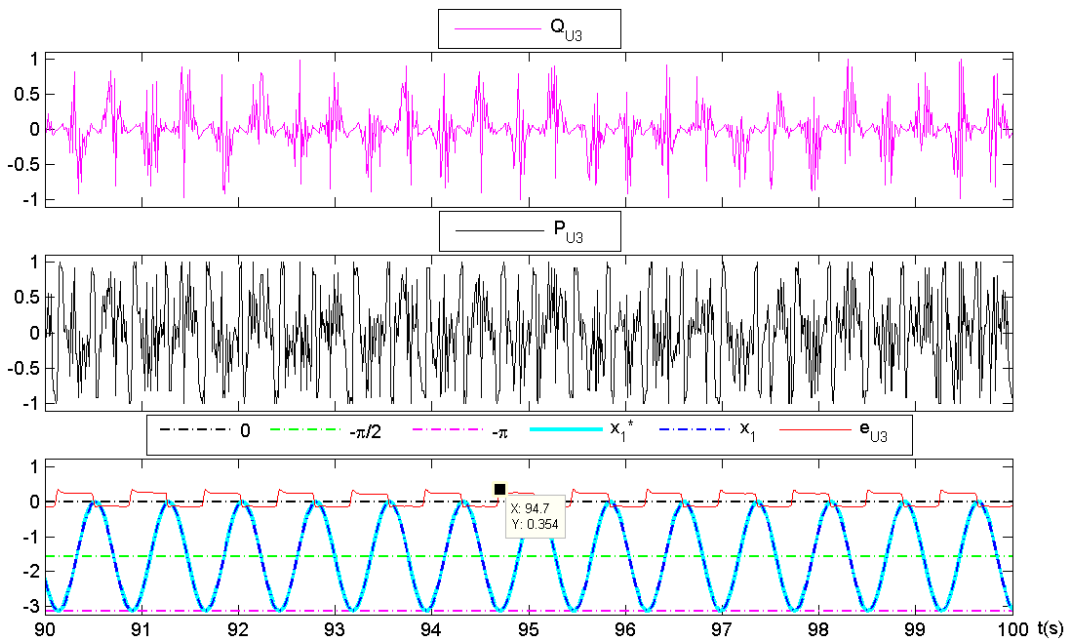


Figure 12 - LQR active control with restriction, noise, uncertainties, amplified at the permanent regime

In Fig. 13 below for the case 3, we can see that due to limitation of maximum pressure and due the uncertainties we obtained peaks that are not more constant as in the case 2, i.e., each time we it happens the reversal of the oscillating motion of the crank.

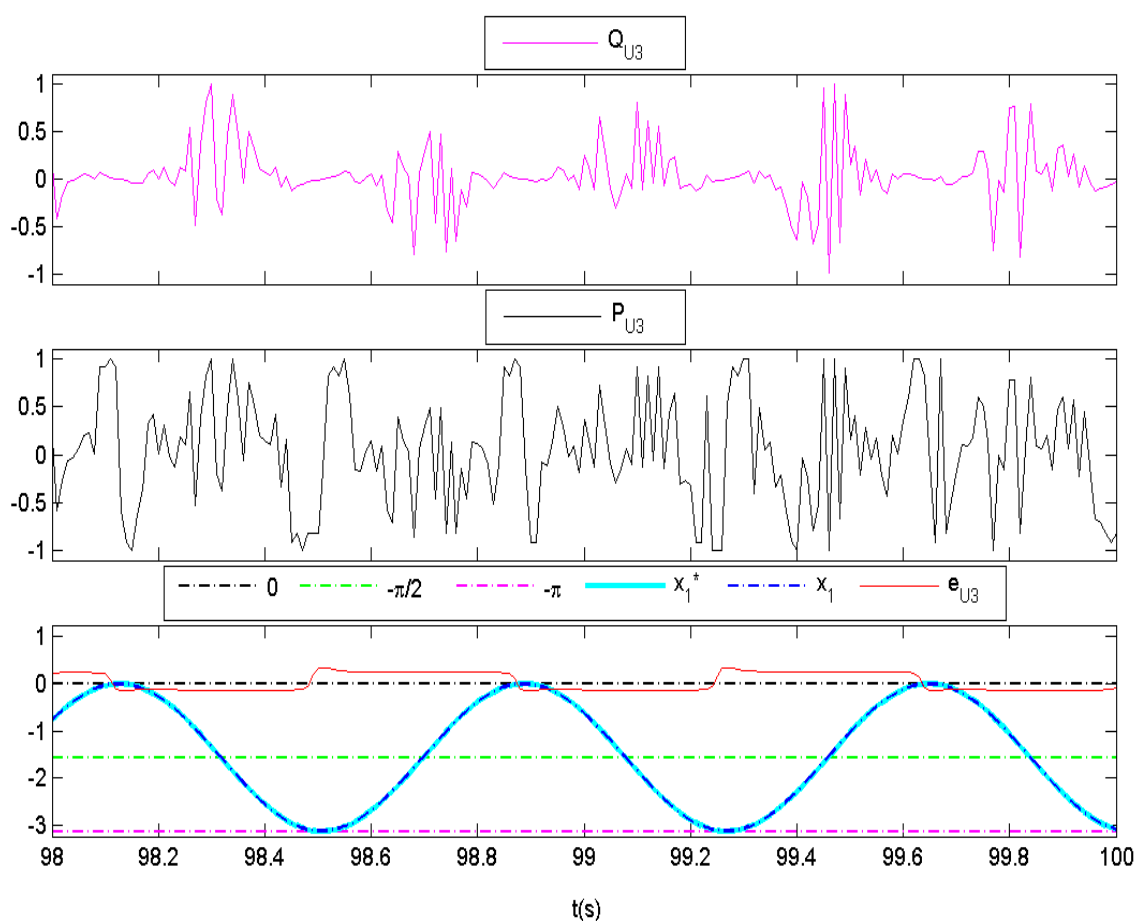


Figure 13 - LQR active control without the saturated pressure and with noise in the permanent regime for the analysis the peaks of the controlled variables

Therefore, the proposed control system has proven robust and efficient for the transient regime or permanent, managing to keep the same parametric error for positions in the case 2 and 3.

3 CONCLUSIONS

This study evaluates the LQR control method for the excitation through pressure in the cylinder of a connecting-rod-crank mechanism as compressed air engine for the controlling the angular oscillation of the crank. Despite the LQR control method in principle being ideal for the use on linear systems this control in the non-linear connecting-rod-crank mechanism also proved for adequate to control the angular oscillation this mechanism.

We evaluated three cases to control the oscillation of the crank between 0 and $-\pi$ for connecting-rod-crank mechanism according to a control function for the desired positions. In first case 1 was not restricted the excitation pressure of which resulted in the saturation of same above the limit for practical application. In second case 2 the excitement by pressure in the cylinder of the connecting-rod-crank mechanism was restricted to a maximum of 1 MPa with the implementation in conjunction of the control function, to facilitate the practical application on commercial pneumatic equipments. In the third case 3 analyses for the error

parametric sensitivity considering uncertainties in the values of pressure, such as the compressibility of the fluid, differences in the friction values, vibrations and noises.

Comparing the parametric errors of the positions in the first case 1 with a saturation pressure with relation the second case 2 without saturation, was verified one increased of the error to 0.001 for the 0.010 rad. However, when applying the saturation control function it is verified that the system gets stable despite the increase of 10^{-3} for 10^{-2} with relationship to error parametric. As for the case 3 even with the uncertainties in the input pressure of the parametric values remained virtually the same error comparing it with the case 2.

The control system has proved robust, even with the inclusion of noise in the entrance of the pressure control variables. The parametric errors obtained are suitable and can be applied to control the angular oscillation of the output to the compressed air engine as a stable system by controlling the saturation. Therefore, the parametric errors around 0.01 radians to the case 2 without signal saturation to the connecting-rod-crank control with the use of simulated parameters are suitable for the application of this mechanism as a compressed air design.

ACKNOWLEDGEMENTS

The authors acknowledge support by CNPq, CAPES, FAPESP and Araucaria Foundation, all Brazilian research funding agencies.

REFERENCES

- Ahmad, F., Hitam, A. L., Hudha, K. & Jamaluddin, H., 2011. Position tracking of slider crank mechanism using PID controller optimized by Ziegler Nichol's method. *Journal of Mechanical Engineering and Technology*, vol. 3. pp. 27-41.
- Alves, A. C., Tusset, A. M., Piccirillo, V., Balthazar, J. M. & Bueno, A. M., 2015. Mathematical model and numerical simulations for control the connecting-rod crankshaft engine with compressed air. *Proceedings of the 23rd ABCM International Congress of Mechanical Engineering / International Conference on Nonlinear Dynamics, Chaos, Control and Applications to Engineering, COBEM 2015 / ICONE 2015*, Rio de Janeiro, pp. 1-8.
- Askari, M. R., Shahrokh, M. & Talkhonch, M. K., 2016. Observer-based adaptive fuzzy controller for nonlinear systems with unknown control directions and input saturation. *Fuzzy Sets and Systems*, 2016.
- Awrejcewicz, J. & Kudra, G., 2003. Modeling and numerical investigation of nonlinear dynamics of a mono-cylinder combustion engine. *Proceedings of DETC'03 Design Engineering Technical Conferences and Computers and Information in Engineering Conference, ASME*, Chicago, Illinois, USA, pp. 1-9.
- Brown, T. L., Atluri, V. P. & Schmiedeler, J. P., 2014. A low-cost hybrid drivetrain concept based on compressed air energy storage. *Applied Energy*, vol. 134, pp. 477-489.
- Chuang, C. W., 2007. PC-based pseudo-model following discrete integral variable structure control of positions in slider-crank mechanisms. *Journal of Sound and Vibration*, vol. 301, pp. 510-520.
- Chuang, C. W., Lee, C. D. & Huang, C. L., 2006. Applying experienced self-tuning PID control to position control of slider crank mechanisms. *Proceedings of the SPEEDAM 2006*,

International Symposium on Power Electronics, Electrical Drives, Automation and Motion, Taormina, Sicily, pp. 652 – 657

Fung, R. F., Chiang, C. L. & Chen, S. J., 2009. Dynamic modelling of an intermittent slider-crank mechanism. *Applied Mathematical Modelling*, vol. 33, pp. 2411–2420.

Galeani, S., Onori, S., Teel, A.R., & Zaccarian, L., 2008. A magnitude and rate saturation model and its use in the solution of a static anti-windup problem. *Systems & Control Letters*, vol. 57, n.1, pp. 1-9.

Hung, Y.-H., Chen, J.-H., Wu, C.-H. & Chen, S.-Y., 2016. System design and mechatronics of an air supply station for air-powered scooters. *Computers & Electrical Engineering*, 2016.

Kao, C. C., Chuang, C. W. & Fung, R. F., 2006. The self-tuning PID control in a slider-crank mechanism system by applying particle swarm optimization approach. *Mechatronics*, vol. 16, pp. 513–522.

Liermann, M., Samhoury, O. & Atshan, S., 2015. Energy efficiency of pneumatic power take-off for wave energy converter. *International Journal of Marine Energy*, 2015.

Lin, F.J., Fung, R.F., Lin, H.H. & Hong, C. M., 2001. A supervisory fuzzy neural network controller for slider-crank mechanism. *Mechatronics*, vol. 11, pp. 227-250.

Noziaki, R. R., Balthazar, J. M. & Tusset, A. M., Pontes JR, B. R. and Bueno, A. M., 2013. Nonlinear control system applied to atomic force microscope including parametric errors. *Journal of Control, Automation and Electrical Systems*, vol. 3, n. 3, pp. 223-231.

Oravec, J. & Bakošová, M., 2015. Robust Model Predictive Control Based on Nominal System Optimization and Control Input Saturation. *IFAC-PapersOnLine*, vol. 48, n. 14, pp. 314-319.

Shaw, D., Yu, J. J. & Chieh, C., 2013. Design of a hydraulic motor system driven by compressed air. *Energies*, vol. 6, n. 7, pp. 3149–3166.

Shi, Y., Wu, T., Cai, M., Wang, Y. & Xu, W., 2016. Energy conversion characteristics of a hydropneumatic transformer in a sustainable-energy vehicle. *Applied Energy*, vol. 171, pp. 77–85.

Tusset, A. M., Bueno, A. M., Nascimento, C. B., Kaster, M. S. & Balthazar, J. M., 2013. Nonlinear state estimation and control for chaos suppression in MEMS resonator. *Shock and Vibration*, vol. 20, pp. 749-761.

Wang, X., Saberi, A. & Stoorvogel, A. A., 2013. Stabilization of linear system with input saturation and unknown constant delays. *Automatica*, vol. 49, n. 12, pp. 3632-3640.

Wang, X., Su, H., Wang, X., & Chen, G. 2016. An overview of coordinated control for multi-agent systems subject to input saturation. *Perspectives in Science*, vol. 7, pp. 133-139.

Wang, Y. W.; You, J. J.; Sung, C. K. & Huang, C. Y., 2014. The Applications of Piston Type Compressed Air Engines on Motor Vehicles. *Procedia Engineering*, vol. 79, pp. 61 – 65.

Yu, Q. & Cai, M., 2015. Experimental Analysis of a Compressed Air Engine. *Journal of Flow Control, Measurement & Visualization*, vol. 3, p. 144-153.

Yu, Q., Shi, Y., Cai, M. & Xu, W., 2016, Fuzzy logic speed control for the engine of an air-powered vehicle. *Advances in Mechanical Engineering*, vol. 8, n. 3, pp. 1–11.

Zheng, Z. & Sun, L., 2016. Path following control for marine surface vessel with uncertainties and input saturation. *Neurocomputing*, vol. 177, pp. 158-167.